



Impact of *in vitro* digestion on gastrointestinal fate and uptake of silver nanoparticles with different surface modifications

Ashraf Abdelkhalik, Meike van der Zande, Anna K. Undas, Ruud J. B. Peters & Hans Bouwmeester

To cite this article: Ashraf Abdelkhalik, Meike van der Zande, Anna K. Undas, Ruud J. B. Peters & Hans Bouwmeester (2020) Impact of *in vitro* digestion on gastrointestinal fate and uptake of silver nanoparticles with different surface modifications, *Nanotoxicology*, 14:1, 111-126, DOI: [10.1080/17435390.2019.1675794](https://doi.org/10.1080/17435390.2019.1675794)

To link to this article: <https://doi.org/10.1080/17435390.2019.1675794>



© 2019 The Author(s). Published by Informa UK Limited, trading as Taylor & Francis Group.



[View supplementary material](#)



Published online: 24 Oct 2019.



[Submit your article to this journal](#)



Article views: 496



[View related articles](#)



[View Crossmark data](#)



Citing articles: 1 [View citing articles](#)

Impact of *in vitro* digestion on gastrointestinal fate and uptake of silver nanoparticles with different surface modifications

Ashraf Abdelkhalik^{a,b,c}, Meike van der Zande^a, Anna K. Undas^a, Ruud J. B. Peters^a and Hans Bouwmeester^b

^aWageningen Food Safety Research, Wageningen, The Netherlands; ^bDivision of Toxicology, Wageningen University, Wageningen, The Netherlands; ^cFood Science and Technology Department, Faculty of Agriculture, Alexandria University, Alexandria, Egypt

ABSTRACT

Nanomaterials, especially silver nanoparticles (AgNPs), are used in a broad range of products owing to their antimicrobial potential. Oral ingestion is considered as a main exposure route to AgNPs. This study aimed to investigate the impact of the biochemical conditions within the human digestive tract on the intestinal fate of AgNPs across an intestinal *in vitro* model of differentiated Caco-2/HT29-MTX cells. The co-culture model was exposed to different concentrations (250–2500 µg/L) of pristine and *in vitro* digested (IVD) AgNPs and silver nitrate for 24 h. ICP-MS and spICP-MS measurements were performed for quantification of total Ag and AgNPs. The AgNPs size distribution, dissolution, and particle concentration (mass- and number-based) were characterized in the cell fraction and in the apical and basolateral compartments of the monolayer cultures. A significant fraction of the AgNPs dissolved (86–92% and 48–70%) during the digestion. Cellular exposure to increasing concentrations of pristine or IVD AgNPs resulted in a concentration dependent increase of total Ag and AgNPs content in the cellular fractions. The cellular concentrations were significantly lower following exposure to IVD AgNPs compared to the pristine AgNPs. Transport of silver as either total Ag or AgNPs was limited (<0.1%) following exposure to pristine and IVD AgNPs. We conclude that the surface chemistry of AgNPs and their digestion influence their dissolution properties, uptake/association with the Caco-2/HT29-MTX monolayer. This highlights the need to take *in vitro* digestion into account when studying nanoparticle toxicokinetics and toxicodynamics in cellular *in vitro* model systems.

ARTICLE HISTORY

Received 5 June 2019
Revised 8 September 2019
Accepted 27 September 2019

KEYWORDS



Silver nanoparticles; surface chemistry; *in vitro* digestion; bioavailability; single particle-ICP-MS


Introduction

Nanomaterials are used in a broad range of products and applications such as textiles, medical devices, water disinfection, personal hygiene and food products (Abdelkhalik et al. 2018; Chaudhry et al. 2008; Imai et al. 2017; Lichtenstein et al. 2015). Because of the antimicrobial potential of silver nanoparticles (AgNPs), they are amongst the most frequently used nanoparticles (NPs) in food associated products (e.g. packaging and kitchen utensils) (Choi et al. 2018; Lichtenstein et al. 2015). Therefore, oral ingestion is considered as a main exposure route for humans to AgNPs. From a risk assessment perspective, understanding the fate, cellular interactions (i.e. cellular uptake) and bioavailability of AgNPs upon digestion

is of key importance to assess their impact on health (Bouwmeester et al. 2011; Hsiao et al. 2016; Lichtenstein et al. 2015, 2017)

Upon oral ingestion of AgNPs, these particles pass through several compartments of the gastrointestinal tract (mouth, stomach and intestine), each with a specific pH and biochemical composition. These varying conditions can affect the AgNPs physicochemical properties (e.g. agglomeration and dissolution) and accordingly affect their bioavailability and toxicological properties (Böhmert et al. 2014; Lichtenstein et al. 2017; Murdock et al. 2008; Sieg et al. 2017). Upon reaching the intestine, the biological interactions (e.g. uptake and transport) of the AgNPs with the intestinal epithelial cells determine their bioavailability and

CONTACT Hans Bouwmeester  hans.bouwmeester@wur.nl  Division of Toxicology, Wageningen University, Stippeneng 4, 6708 WB Wageningen, The Netherlands

 Supplemental data for this article can be accessed [here](#).

This article has been republished with minor changes. These changes do not impact the academic content of the article.

© 2019 The Author(s). Published by Informa UK Limited, trading as Taylor & Francis Group.

This is an Open Access article distributed under the terms of the Creative Commons Attribution-NonCommercial-NoDerivatives License (<http://creativecommons.org/licenses/by-nc-nd/4.0/>), which permits non-commercial re-use, distribution, and reproduction in any medium, provided the original work is properly cited, and is not altered, transformed, or built upon in any way.

possible subsequent systemic effects upon oral ingestion (McCracken et al. 2015). AgNPs size and surface chemistry play an important role in their stability, cellular internalization, and transport (Lichtenstein et al. 2017; Mwilu et al. 2013). Several *in vitro* models have been developed to represent the intestinal epithelial barrier (Lefebvre et al. 2015) which are exposed to NPs to simulate real-life human exposure conditions to NPs (Nel et al. 2006; Sieg et al. 2017). Among these model, the co-cultures of monolayers of Caco-2 intestinal cells and HT29-MTX mucus secreting cells are widely used as an *in vitro* intestinal epithelium model (Bailey, Bryla, and Malick 1996; Georgantzopoulou et al. 2015; Lefebvre et al. 2015; Stone, Johnston, and Schins 2009). These models however do not consider possible effects of digestion on toxicokinetics and toxicodynamics of NPs.

Detection, characterization, and quantification of (metal) nanoparticles are of importance in studying the fate of NPs. For this, several analytical methods have been developed (López-Serrano et al. 2014). Single particle-inductively coupled plasma mass spectrometry (spICP-MS) has shown high efficacy and sensitivity to detect NPs at low concentrations in addition to its ability to distinguish between metal ions and NPs (Abdolapur Monikh et al. 2019; Ding et al. 2018; van der Zande et al. 2016; Weigel et al. 2017). In addition, spICP-MS provides information on the size, size distribution, and mass- and number-based NPs concentration (Hsiao et al. 2016; Laborda et al. 2011; Peters et al. 2015). To study the cellular uptake and internalization of AgNPs, however, additional techniques need to be used. For this we used confocal fluorescence microscopy exploiting the light scattering properties of AgNPs in combination with immunohistochemistry (Kittler et al. 2010; van der Zande et al. 2016). Here, we aimed to investigate the impact of *in vitro* digestion (IVD) on two 50 nm AgNPs with different surface chemistries, while silver nitrate (AgNO_3) was used as an ionic control. An *in vitro* human digestion model was used to mimic the oral, gastric, and small intestinal conditions (Lichtenstein et al. 2015; Versantvoort et al. 2005; Walczak et al. 2012). The size, size distribution, dissolution, and particle concentration (mass- and number-based) of the AgNPs after *in vitro* digestion using spICP-MS and ICP-MS were measured and quantified.

Also, we investigated the impact of *in vitro* digestion on the uptake/association and transport of the

AgNPs in or through the intestinal barrier using an *in vitro* Caco-2 and HT29-MTX co-culture transwell model.

Materials and methods

Nanoparticles and chemicals

Two 50 nm negatively charged AgNPs with different surface modifications were purchased from Nanocompositix Inc. (San Diego, CA, USA); lipoic acid BioPure™ (pH 6.1) in milli-Q water and citrate BioPure™ (pH 7.4) in 2 mM citrate buffer, further referred to as (LA) and (Cit) AgNPs, respectively. The silver mass concentration in the stock suspensions of both AgNPs was 1 mg/mL. All the AgNPs suspensions were stored at 4 °C in the dark. Dilutions of the AgNPs were freshly prepared for every experiment in complete cell culture medium (DMEM⁺), prepared by supplementing Dulbecco's Modified Eagle Medium (DMEM) culture medium (LONZA, Basel, Switzerland) with 10% (v/v) heat inactivated Fetal Bovine Serum (FBS) (Gibco®, Life technologies, USA), 1% (v/v) of Penicillin–Streptomycin 10 000 units penicillin, and 10 mg streptomycin/mL (Sigma-Aldrich, St Louis, MO, USA), and 1% (v/v) of MEM Non-Essential Amino Acids (NEAA) (Gibco®, life technologies, Langley, OK, USA). Silver nitrate (AgNO_3) (Sigma, USA) was used as a control (source of Ag^+ ions) in all the experiments. Dilutions of AgNO_3 were freshly prepared for every experiment in DMEM⁺.

Physicochemical characterization of nanoparticles

Hydrodynamic diameters of AgNPs were determined using dynamic light scattering (DLS). Measurements were performed on samples containing 10 mg/L AgNPs suspended in nano-pure water using an ALV dynamic light scattering setup (ALV-Laser Vertriebsgesellschaft, Langen, Germany), consisting of a Thorn RFIB263KF photomultiplier detector, an ALV-SP/86 goniometer, an ALV 50/100/200/400/600 μm pinhole detection system, an ALV7002 external correlator, and a Cobolt Samba-300 DPSS laser. Measurements were performed at $t=0$ h and at $t=24$ h at room temperature, samples were incubated at 37 °C. For each condition, samples were analyzed in triplicate; each measurement consisted of 10 technical replicates measurements of 30 s each, at an angle of 90°. The results are expressed as the average

hydrodynamic diameter (nm) \pm standard deviation (SD) that was calculated using AfterALV[®] software (AfterALV 1.0d, Dullware, USA).

The AgNPs surface charges were determined by measuring the zeta-potential of 10 μ g/mL AgNPs suspensions in nano-pure water using a Malvern Nanosizer (Malvern Instruments, UK). All samples were analyzed in triplicate.

The total silver content of pristine AgNPs suspensions and AgNO₃ solution was analyzed using a NexION 350 D (PerkinElmer, Waltham, MA, USA) ICP-MS. Before analysis, samples were digested using an aqua-regia [1:3 (v/v), 70% HNO₃: 37% HCl] acid digestion for 30 min at 60 °C and diluted with nano-pure water. Silver was measured using the selected element-monitoring mode with *m/z* values of 107 and 109. A matrix-matched calibration curve of an ionic Ag standard (AgNO₃) (Merck, Darmstadt, Germany) ranging from 0.1 to 50 μ g/L was included. Rhodium (Merck, Germany) was used as an internal standard. The limit of detection (LOD_{conc}) and limit of quantification (LOQ_{conc}) were 4 and 13.5 ng/L respectively and they were calculated by the measurement of blank samples as mass concentration in the blank + 3 \times SD and 10 \times SD respectively. All samples were analyzed in triplicate.

The particle size, size distribution, mass- and number-based particle concentration of pristine AgNPs suspensions and AgNO₃ solution were quantified using spICP-MS. The method for the spICP-MS measurements was described previously (Peters et al. 2015). Briefly, the sample flow rate to the nebulizer was determined before the start of each series of measurements. The dwell time was set at 3 ms and the total acquisition time was set at 60 s. A diluted suspension of 60 nm gold NPs

(Nanocomposix, USA) with a mass concentration of 50 ng/L was used before each analysis to verify the performance of the ICP-MS and to determine the transport efficiency. A calibration curve of ionic silver (AgNO₃) with a concentration range of 0.1–20 μ g/L was used. The time scan data of the spICP-MS measurements were exported as .csv files, and the calculation of the particle size, size distribution, and mass- and number-based concentrations from the spICP-MS data were performed using a dedicated spreadsheet. Details about the spreadsheet have been described previously (Peters et al. 2015). The LOD_{conc} and LOQ_{conc} were estimated to be 22 and 75 ng/L respectively and they were calculated by the measurement of blank samples as mass concentration in the blank + 3 \times SD and 10 \times SD respectively. The NP size was calculated based on the particle mass, assuming spherical particles. The size detection limit (LOD_{size}) was 20 nm and accordingly any silver particles with sizes below this limit were included in the ionic silver fraction.

In vitro digestion of AgNPs and AgNO₃

The two AgNPs suspensions and the AgNO₃ solution were digested using an *in vitro* human gastrointestinal digestion model with a pH gradient ranging from 7 (mouth), to 5 (stomach), to 7 (intestine). The pH of 5 in the stomach is meant to resemble the conditions upon food consumption which leads to a decrease of stomach acidity, opposed to a pH of \sim 2 under fasted conditions (Minekus et al. 2014). Briefly, all digestive juices were freshly prepared and warmed to 37 °C before use as described in Table 1 (Versantvoort et al. 2005; Walczak et al. 2012).

Table 1. Composition of the artificial digestion fluids of the *in vitro* digestion model (per 1000 mL) (Versantvoort et al. 2005; Walczak et al. 2012).

Saliva (pH 6.8 \pm 0.1)	Gastric fluid (pH 1.3 \pm 0.1)	Duodenal fluid (pH 8.1 \pm 0.1)	Bile fluid (pH 8.2 \pm 0.1)
<ul style="list-style-type: none"> • 896 mg KCl • 200 mg KSCN • 1021 mg NaH₂PO₄·H₂O • 570 mg Na₂SO₄ • 298 mg NaCl • 1694 mg NaHCO₃ • 200 mg urea • 290 mg amylase • 15 mg uric acid • 25 mg mucin • Nano-pure water 	<ul style="list-style-type: none"> • 2752 mg NaCl • 306 mg NaH₂PO₄·H₂O • 824 mg KCl • 302 mg CaCl₂ • 306 mg NH₄Cl • 6.5 mL 37% HCl • 650 mg glucose • 20 mg glucuronic acid • 85 mg urea • 330 mg glucosamine-hydrochloride • 1 g BSA • 2.5 g pepsin • 3 g mucin • Nano-pure water 	<ul style="list-style-type: none"> • 7012 mg NaCl • 3388 mg NaHCO₃ • 80 mg KH₂PO₄ • 564 mg KCl • 50 mg MgCl₂·6H₂O • 180 mL HCl (37%) • 100 mg urea • 151 mg CaCl₂ • 1 g BSA • 9 g pancreatin • 1.5 g lipase • Nano-pure water 	<ul style="list-style-type: none"> • 5259 mg NaCl • 5785 mg NaHCO₃ • 376 mg KCl • 150 mL HCl (37%) • 250 mg urea • 167.5 mg CaCl₂ • 1.8 g BSA • 30 g bile • Nano-pure water Sodium carbonate solution • 84.7 g NaHCO₃ • Nano-pure water

A volume of 1 mL, with a concentration of 500 mg/L of AgNPs suspensions or 95 mg/L AgNO₃ solution, was mixed with 3 mL of saliva (pH 6.8±0.1) and incubated (head-over-heads at 55 rpm) for 5 min at 37 °C to simulate the digestion in the mouth. Subsequently, 6 mL of gastric juice (pH 1.3±0.1) was added to the mixture and the pH was checked and adjusted to 5±0.5 with NaOH (5 M) to simulate the digestion in the stomach. The samples were further incubated while rotating at head-over-heads at 37 °C for 2 h. Lastly, 6 mL of duodenal juice (pH 8.1) and 3 mL of bile (pH 8.2) were added to the mixture and the pH was checked and adjusted to 6.5±0.5 with NaOH (1 M) or HCl (37%) to simulate the digestion in the small intestine. Again, the samples were incubated while rotating head-over-heads at 37 °C for 2 h. The complete mixture of all the digestive juices is further referred to as chyme.

The total silver content of the IVD AgNPs suspensions and AgNO₃ solution was analyzed using ICP-MS as described earlier. spICP-MS measurements were used to quantify the particle size, size distribution, and mass- and number-based concentrations of the IVD AgNPs suspensions and AgNO₃ solution as described earlier. The silver ions calibration curves were prepared in a similar matrix as the samples of interest.

Cell culture

A co-culture of adherent human epithelial colorectal adenocarcinoma cells (Caco-2; ATCC[®] HTB-37[™]; USA) and human colon adenocarcinoma mucus secreting cells (HT29-MTX; ECACC, Ireland) was prepared of cells at passage numbers of 25–40 and 8–40, respectively. Both cell lines were cultured and separately maintained in 75 cm² cell culture flasks (Corning[®]; Corning, NY, USA) at 37 °C in a humidified 5% CO₂ atmosphere in DMEM⁺.

Cell viability

Cytotoxic effects of the pristine and IVD AgNPs and AgNO₃ were determined using the WST-1 cell viability assay (Roche, Basel, Switzerland). Each well was seeded with 100 µL of a 1 × 10⁵ cells/mL suspension with a 3:1 ratio Caco-2: HT29-MTX in DMEM⁺ in 96-well flat bottom plates (Grenier bio-one, Alphen aan

den Rijn, The Netherlands). Plates were incubated at 37 °C, 5% CO₂ for 24 h. The attached cells were then exposed to 100 µL/well of freshly prepared dilutions (100–100,000 µg/L) of pristine and (500–2500 µg/L) IVD AgNPs suspensions and/or (125–500 µg/L) AgNO₃ solution. All the IVD AgNPs and AgNO₃ dilutions had a 9:1 DMEM⁺: chyme ratio, to prevent toxicity of the chyme. After 24 h of exposure, the exposure medium was discarded, and the cells were washed once with 100 µL/well HBSS buffer before addition of 10 µL of WST-1 solution with 90 µL of DMEM⁺ (without phenol red) to each well. The plates were incubated for 4 h at 37 °C, 5% CO₂ and absorbance was read at 490 and 630 nm on a plate reader (BioTek Synergy[™] HT Multi-Mode Microplate reader, Winooski, VT, USA). The cell viability was expressed as % of control. DMEM⁺ was used as a negative control and Triton-X100 (0.25%) (Sigma) was used as a positive control.

In vitro intestinal monolayer barrier integrity assessment

The Caco-2 and HT29-MTX cells were grown in a ratio of 3:1 (Kleiveland 2015; Walczak, Kramer, Hendriksen, Helsdingen, et al. 2015a) at a density of 4 × 10⁴ cells/cm² on the upper side of transwell polyester inserts (0.4 µm pore size, 1.12 cm² surface area) (Corning, USA) for 21 days. The integrity of the monolayer was assessed before AgNPs exposure by measuring the transepithelial electrical resistance (TEER) values using a Millicell ERS-2 Epithelial Volt-Ohm Meter (Millipore, USA). On day 21, only inserts with TEER values above 200 Ω.cm² before exposure were used. In addition, a maximum of 20% reduction in TEER values was accepted after exposure.

Additionally, the transport efficacy of each of three different integrity markers namely; lucifer yellow (LY) (Sigma, USA) and low (4 kDa) and high (10 kDa) molecular weights fluorescein isothiocyanate dextrans (FITC-D) (Sigma, USA) was evaluated in the presence and absence of EGTA (a tight-junction disruptor) (Sigma, USA) to assess the cell monolayer integrity. In the absence of EGTA, 500 µL/insert of 1 mg/mL in DMEM⁺ of the integrity markers were added apically. After 1 h incubation at 37 °C, the basolateral medium was collected, and the transport of the markers was determined by measuring the fluoresce at 485/530 nm using the fluorescence

plate reader. For samples evaluated in the presence of EGTA, 500 μL of a solution of 2.5 mM EGTA/DMEM⁺ was added apically and basolaterally followed by incubation of the monolayers for 1 h at 37 °C. The wells were then refreshed with 2.5 mM EGTA/DMEM⁺ solution in the basolateral compartment while apically the integrity markers in DMEM⁺ were added at a concentration of 1 mg/mL. The cells were incubated for 1 h at 37 °C and the basolateral medium was collected and analyzed for the presence of the markers as described above.

Cellular uptake/association and transport of AgNPs and AgNO₃

The cellular monolayer was exposed apically to 500 μL /insert of 250, 500, and 2500 $\mu\text{g/L}$ of pristine or IVD AgNPs suspensions and to 250 $\mu\text{g/L}$ of pristine or IVD AgNO₃ solutions for 24 h at 37 °C, 5% CO₂. Then, the media from the apical and basolateral compartments were collected and the cells were collected by trypsinization and sonication (40 kHz for 15–20 min) to lyse the cells. The total silver content of all the samples was analyzed using ICP-MS as described earlier. spICP-MS was used to quantify the particle size, size distribution, and mass- and number-based concentrations of all samples as described above.

Confocal microscopy

For confocal imaging, Caco-2/HT29-MTX co-cultures were cultured in transwells and exposed to both pristine and IVD AgNPs suspensions and AgNO₃ solution using similar conditions as used in the uptake/association and transport experiments. After exposure, the exposure medium was discarded, and the cells were fixed with 4% paraformaldehyde (Sigma, USA) for 15 min. The cells were washed 3 times with PBS for 5 min after discarding the fixation solution. The cells were permeabilized with 0.25% Triton X-100/PBS for 15 min. The cells were then washed again 3 times with PBS for 5 min before incubating them with the blocking buffer (1% BSA in PBS) for 30 min. After discarding the blocking buffer, Phalloidin – Alexa 488 (6 units) (Dyomics, Germany) was added to stain cellular actin and the cells were incubated for 30 min. Cells were washed three times with PBS before

incubating the cells for 10 min with RedDot-2 (1:200) (Biotium, USA) to stain the nuclei. Finally, the cells were washed with PBS and stored in the dark until analysis. The cells were analyzed using a confocal laser scanning microscope (SP5X-SMD; Leica Microsystems, Germany). Samples were excited with 665 and 495 nm lasers and backscattered light was used to detect AgNPs using a 543 nm laser. All preparations steps have been done at room temperature.

Transmission electron microscopy energy-dispersive spectroscopy (TEM-EDS) analysis

Following the 24 h exposure of the Caco-2/HT29-MTX co-culture to pristine or IVD AgNPs or AgNO₃, samples from the basolateral compartments were withdrawn. The samples were deposited on a holey carbon coated Cu TEM grid (Agar Scientific, UK) and dried at room temperature before examination using a TEM-EDS system. The grid examination was performed on a JEM-2100 equipped with EDS system of OI Aztec 80 mm X-max detector.

Statistical analysis

Each data point of all the experiments performed represents the average from three replicates ($n=3$) and the results are shown as mean \pm standard deviation after analysis by Prism[®] (v.8.0.1; GraphPad[®], USA) software. Bonferroni's post-test was used to test statistical significance upon performing a one-way analysis of variance (ANOVA). A p -value < 0.05 was considered significant.

Results

Physicochemical characterization of the pristine AgNPs suspensions and AgNO₃ solution

Two differently coated AgNPs were used in this study: lipoic acid-coated (LA) AgNPs and citrate-coated (Cit) AgNPs. The nominal sizes provided by the supplier of the (LA) and (Cit) AgNPs measured by transmission electron microscopy (TEM) were 51 ± 5 and 52 ± 6 nm, respectively. The hydrodynamic sizes and the ζ – potential of both AgNPs, measured in nano-pure water after 0 and 24 h incubation at 37 °C, are listed in Table 2. There were no

Table 2. Physicochemical characteristics of AgNPs.

Medium	Incubation time (h)	Hydrodynamic diameter (nm) \pm SD		ζ -potential (mV) \pm SD	
		(LA) AgNPs	(Cit) AgNPs	(LA) AgNPs	(Cit) AgNPs
Nano-pure water	0	56 \pm 8	51 \pm 1	-56 \pm 10	-37 \pm 7
	24	49 \pm 2	48 \pm 4	-36 \pm 10	-29 \pm 12

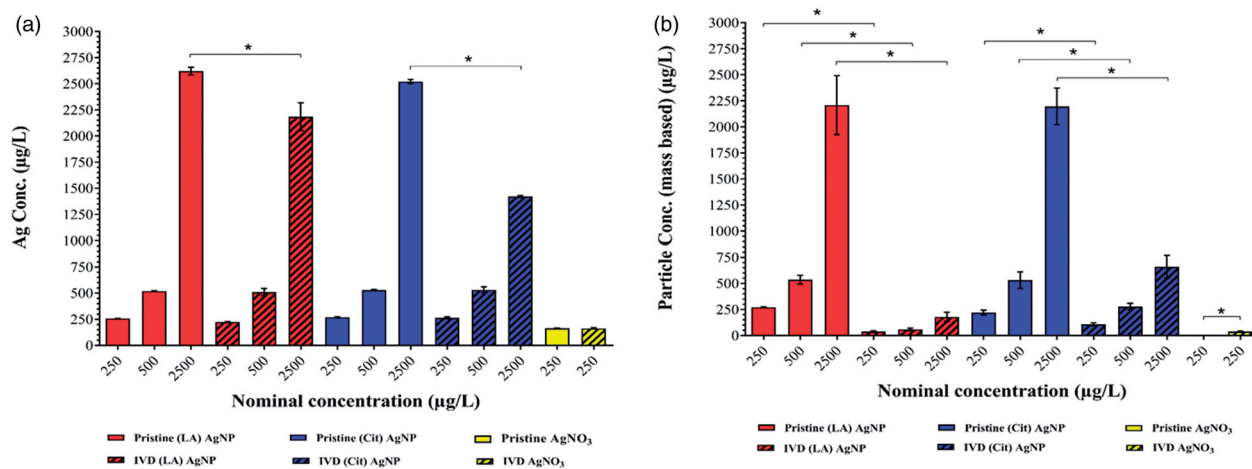


Figure 1. Silver content in pristine and *in vitro* digested (IVD) AgNPs suspensions and AgNO₃ solution. (a) Silver content measured as total Ag using ICP-MS. (b) Silver content measured as AgNPs using spICP-MS. Concentrations are given as the mean \pm SD ($n = 3$). *Significant difference between the pristine and IVD suspension of the same AgNPs ($p < 0.05$).

significant differences in the hydrodynamic diameters or the charges of both AgNPs over time.

The suspensions of both AgNPs and AgNO₃ were analyzed as pristine suspensions and after *in vitro* digestion (IVD suspensions) to quantify the total silver content and silver in particulate form (AgNPs) using ICP-MS and spICP-MS, respectively (Figure 1).

The AgNPs content in the pristine suspensions of both types of AgNPs was equal to the total Ag content and corresponded to the theoretical (nominal) concentration. The pristine solution of AgNO₃ did not contain detectable levels of AgNPs.

Upon IVD, the total Ag content of both AgNPs suspensions and the AgNO₃ solution remained unchanged (compared to the pristine suspension) except the highest concentration of AgNPs (Figure 1(a)). The AgNPs content of both types of AgNPs was significantly reduced upon digestion at all concentrations tested. The IVD (LA) AgNPs suspension showed a reduction in particulate silver (mass-based) between 86 and 92% while the IVD (Cit) AgNPs suspension showed a reduction between 48 and 70% in particulate silver (mass-based), compared to the pristine suspensions. Interestingly, a low but significantly elevated concentration of newly formed silver particulates (*de novo*) was observed in the AgNO₃ solution upon digestion (Figure 1(b)).

Assessment of AgNPs and AgNO₃ cytotoxicity

The viability of the Caco-2/HT29 co-culture was assessed using the WST-1 assay (cellular mitochondrial activity determination) upon 24 h exposure to increasing concentrations of pristine or IVD AgNPs suspensions and AgNO₃ solution (Figure 2). The pristine AgNO₃ induced concentration dependent cytotoxicity. The cell viability of all the concentrations used in the subsequent experiments of pristine or IVD AgNPs suspensions (up to 2500 µg/L) and AgNO₃ solution (up to 500 µg/L) was higher than 85%.

Cellular barrier integrity assessment

For the transport studies, monolayers of Caco-2/HT29-MTX coculture were grown for 21 days in transwells to allow cells to form a tight junction and differentiated monolayer. Only monolayers that had TEER values $> 200 \Omega \cdot \text{cm}^2$ were used for subsequent cellular uptake/association and transport studies. The monolayer integrity was also confirmed by assessing the transport of lucifer yellow (LY), and 4 kDa and 10 kDa FITC-dextran in the presence or absence of a tight junction disruptor (EGTA). The transport of the three markers was very limited ($< 0.5\%$) in the absence of the EGTA, while upon addition of EGTA

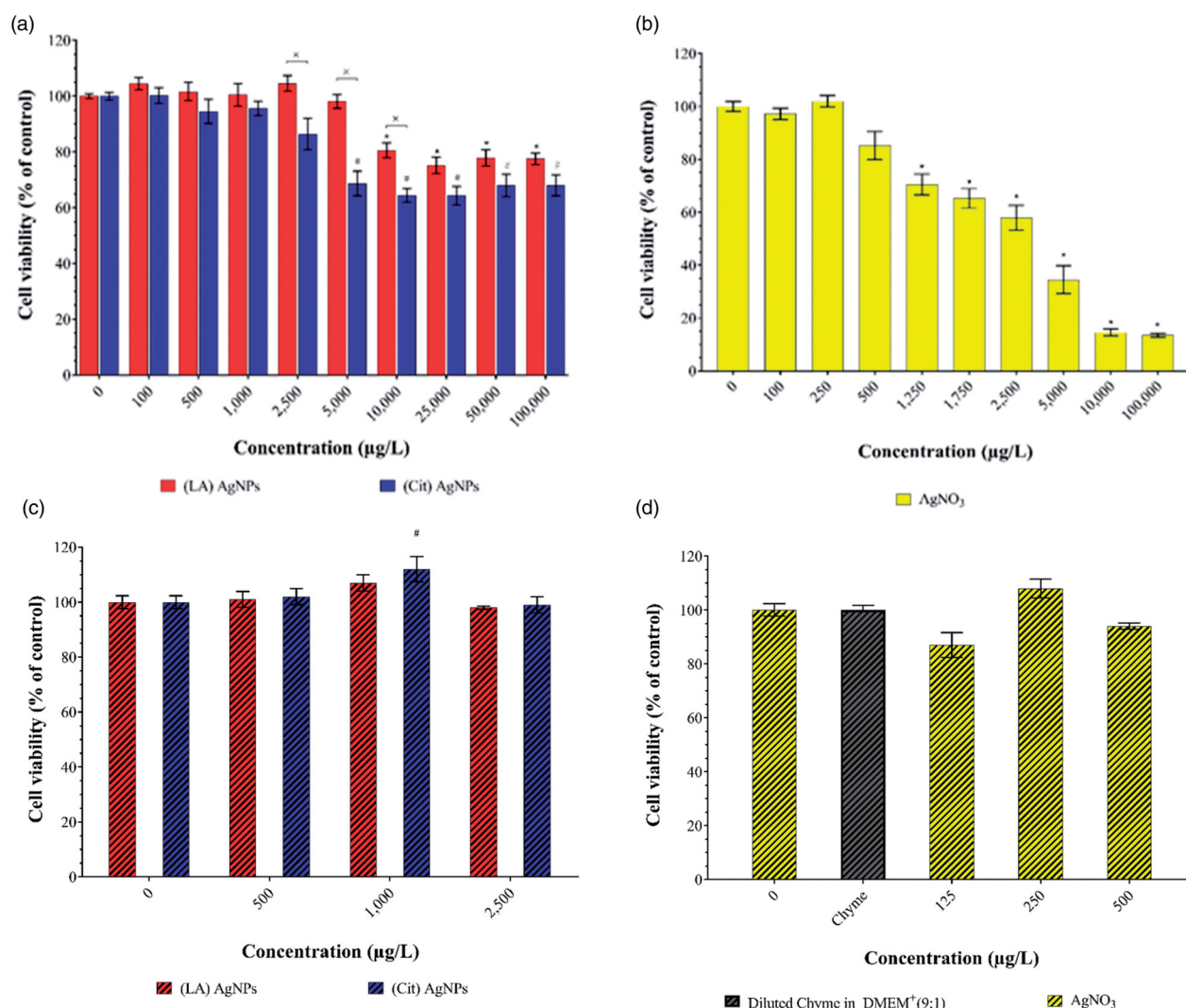


Figure 2. Cell viability of a Caco-2/HT29-MTX co-culture after 24 h exposure to a concentration range of pristine: (a) (LA) and (Cit) AgNPs and (b) AgNO₃, and IVD; (c) (LA) and (Cit) AgNPs and (d) AgNO₃ using the WST-1 viability assay. Viability is given as a percentage of the control (mean ± SD; $n = 3$). ^xSignificant difference between AgNPs at the same concentration ($p < 0.05$). ^{*}[#]Significant difference between any concentration and the control within the same treatment ($p < 0.05$).

the transport increased significantly (up to 20- to 140-fold) (Supplementary Material, Figure S1).

Cellular uptake/association of AgNPs and AgNO₃ by monolayers of intestinal epithelial cells

Monolayers of 21 days old Caco-2/HT29-MTX coculture were exposed for 24 h to increasing concentrations of either pristine or IVD AgNPs suspensions or AgNO₃ solution. The resulting cellular uptake/association of Ag was quantified and expressed as total Ag and AgNPs (Figure 3).

The total Ag and AgNPs content in the cell fraction increased in a concentration-dependent manner for both AgNPs irrespective of their treatment (pristine or IVD) (Figure 3). Upon the pristine AgNPs

exposure, the total Ag contents in the cellular fraction of (LA) AgNPs samples were significantly higher than that in the (Cit) AgNPs samples (Figure 3(a)). While the cellular fraction content of AgNPs exposed to (LA) AgNPs was significantly higher at the highest concentration compared to (Cit) AgNPs samples (Figure 3(b)). After IVD, comparable levels of Ag and AgNPs were detected in the (LA) and (Cit) AgNPs samples except for the highest concentration where the (Cit) AgNPs samples had a significant higher Ag and AgNPs concentrations than the (LA) AgNPs samples (Figure 3(c,d)).

In the cell fraction samples upon exposure to both pristine and IVD AgNO₃, mainly total Ag was detected, but after IVD a limited number of AgNPs was detected.

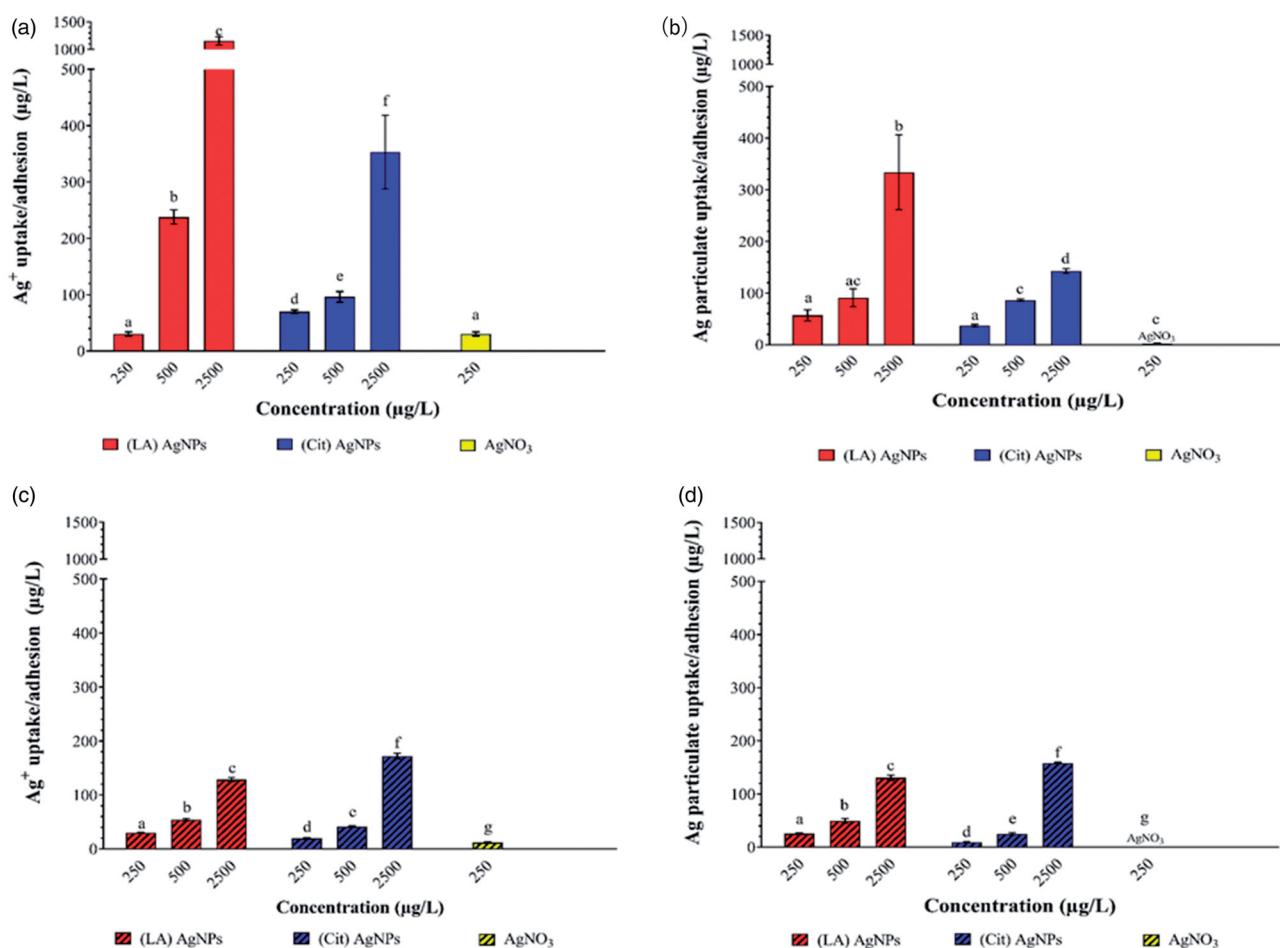


Figure 3. Silver uptake/adhesion of (LA) and (Cit) AgNPs and AgNO₃ in differentiated Caco-2/HT29-MTX cells after 24 h exposure, measured and expressed as total Ag after (a) exposure to pristine AgNPs and AgNO₃; (c) exposure to *in vitro* digested AgNPs and AgNO₃. Also expressed as AgNPs after (b) exposure to pristine AgNPs and AgNO₃; (d) exposure to *in vitro* digested AgNPs and AgNO₃. Concentrations are given as the mean \pm SD ($n = 3$). Values with different letters are significantly different at the same concentration ($p < 0.05$).

In general, the cellular silver contents as total Ag or AgNPs upon exposure to IVD AgNPs was significantly lower compared to exposure to pristine AgNPs. Confocal microscopy was applied to evaluate cellular internalization of both AgNPs (pristine or IVD). Various planes through the cells were assessed showing that clusters of silver or AgNPs were mainly localized in the cytoplasm and to some extent in the nucleus (Figure 4).

Transport of AgNPs and AgNO₃ across monolayers of intestinal epithelial cells

The transport of either pristine or IVD AgNPs and AgNO₃ through the Caco-2/HT29-MTX monolayers was minimal (<0.1%) either as total Ag or AgNPs. Also, using TEM-EDS no AgNPs could be detected in samples from the basolateral compartments in

any of the exposure groups. Only in small areas of the examined grids, an increased number of silver counts were found, but they were not visible in a particulate form (data not shown).

spICP-MS size distribution in pristine and IVD suspensions

The spICP-MS measurements were transformed into size distribution plots depicting the number of particles corresponding to each AgNPs diameter cluster (5 nm) on y- and x-axis, respectively (Figure 5). The number of particles measured in the AgNPs suspensions and AgNO₃ solution are presented in Supplementary Material, Table S1. There was no apparent difference in the size distributions of the pristine suspensions of both AgNPs, with a median size of 50 nm (Figure 5(a,b)). No AgNPs could be

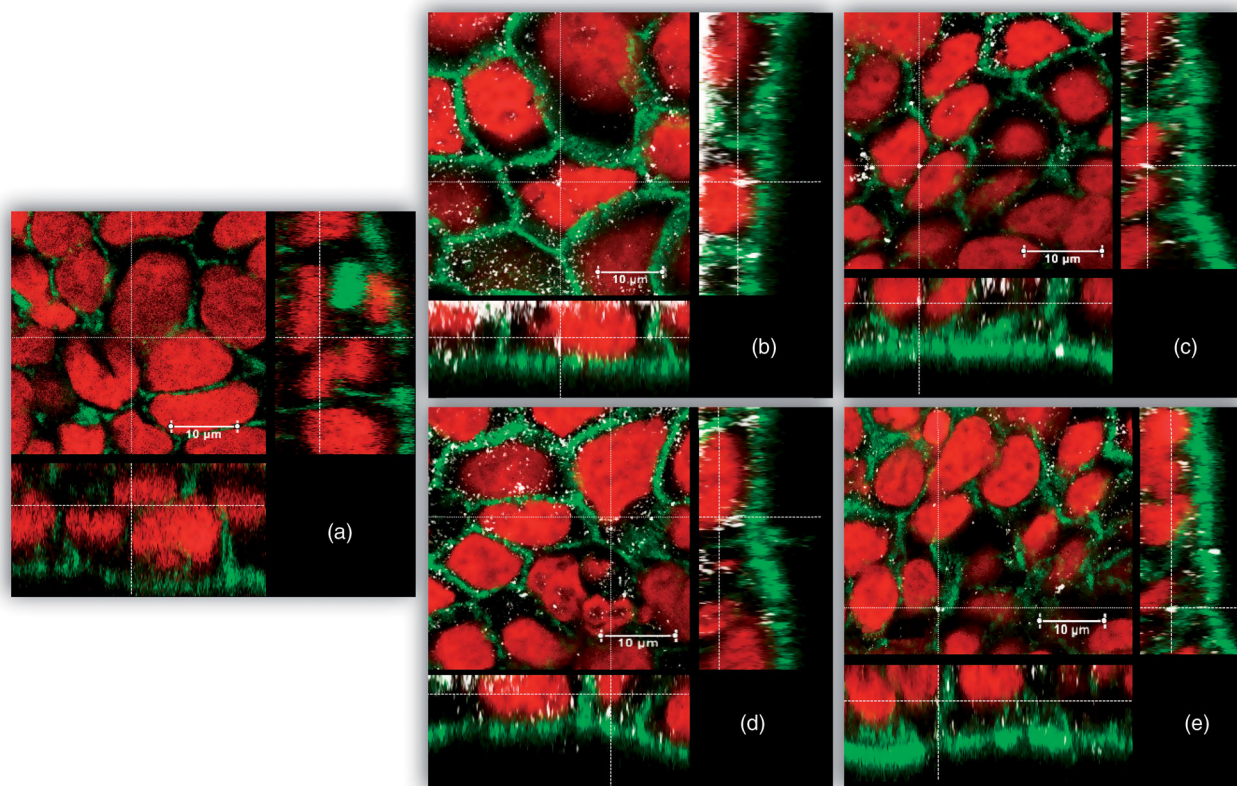


Figure 4. Uptake/adhesion of AgNPs after 24 h exposure. Confocal microscopy images of 21-day-old Caco-2/HT29-MTX cells. (a) without exposure to AgNPs (negative control), after exposure to 2500 µg/L, (b) pristine (LA) AgNPs, (c) pristine (Cit) AgNPs, (d) IVD (LA) AgNPs, and (E) IVD (Cit) AgNPs. Nuclei were stained in red (RedDot-2), actin was stained in green (Alexa-488 Phalloidin) and AgNPs are shown in white (back scatter).

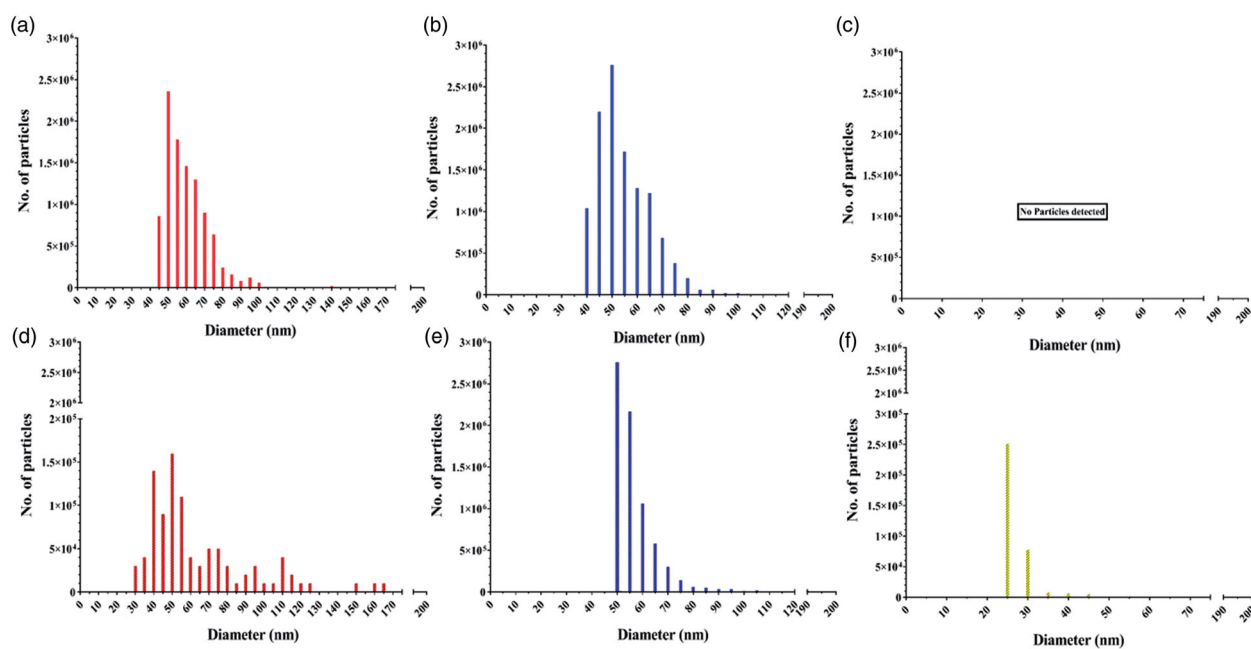


Figure 5. Number-weighted size distributions generated by spICP-MS measurements in exposure suspensions. (a) 500 µg/L pristine (LA) AgNPs, (b) 500 µg/L pristine (Cit) AgNPs, (c) 250 µg/L pristine AgNO₃, (d) (LA) 500 µg/L IVD AgNPs, (e) 500 µg/L IVD (Cit) AgNPs, and (f) 250 µg/L IVD AgNO₃.

detected in the pristine solution of AgNO_3 (Figure 5(c)).

In vitro digestion affected the size and size distribution of (LA) AgNPs, as the mass-concentration were reduced ($\sim 90\%$ lower) compared to the pristine samples (Figure 5(d); also reflected in Figure 1). In addition, the size distribution curves of the IVD suspensions showed broadened distributions, indicating the presence of both smaller and larger particles. The size distribution of the (Cit) AgNPs was less affected by *in vitro* digestion, where the majority of both the pristine and IVD (Cit) AgNPs had a median size of 50 nm (Figure 5(b,e)). The total number of particles was reduced ($\sim 38\%$ lower) compared to the pristine particles. Upon *in vitro* digestion, newly formed silver particulates (*de novo*) were found in the AgNO_3 solution with a median size of 25 nm (Figure 5(f)). All the size distributions of the three concentrations of AgNPs were following similar trend, accordingly all the size distributions reported in Figure 5 are only for of 500 $\mu\text{g/L}$ of AgNPs and 250 $\mu\text{g/L}$ AgNO_3 for simplicity and clarity purposes.

spICP-MS size distribution in cellular fraction

The size distributions (Figure 6) and number of particles (Supplementary Material, Table S1) of both

AgNPs measured in the cellular fraction were different depending on the surface chemistry of the AgNPs and on whether they were pristine or IVD. Following exposure to pristine (LA) AgNPs, a broad size distribution was observed without a clear peak (Figure 6(a)). This distribution was highly different from the size distribution in the pristine suspension (Figure 5(a)). For the pristine (Cit) AgNPs, the cellular fraction has AgNPs with a median size of 35 nm and the size distribution (Figure 6(b)) was comparable to that of the pristine (Cit) AgNPs suspension (Figure 5(b)). Among pristine AgNPs, the number of NPs in the cell fraction exposed to (LA) AgNPs ($3.1 \times 10^5 \pm 4.6 \times 10^4$) was significantly lower than the number of particles detected in the cells exposed to (Cit) AgNPs ($2.6 \times 10^6 \pm 1.7 \times 10^5$).

The size distribution of IVD (LA) AgNPs in the cell fraction – compared to the IVD suspension distribution of these AgNPs (Figure 5(d)) – was right skewed with a median size of 45 nm (Figure 6(d)). The broadening of the size distribution and longer tail showed the appearance of bigger particles (aggregates) up to 200 nm. The size distribution of IVD (Cit) AgNPs in the cell fraction (Figure 6(e)) also showed a longer tail compared to the IVD (Cit) AgNPs suspension (Figure 5(e)), showing bigger particles (aggregates) up to 200 nm with a median size

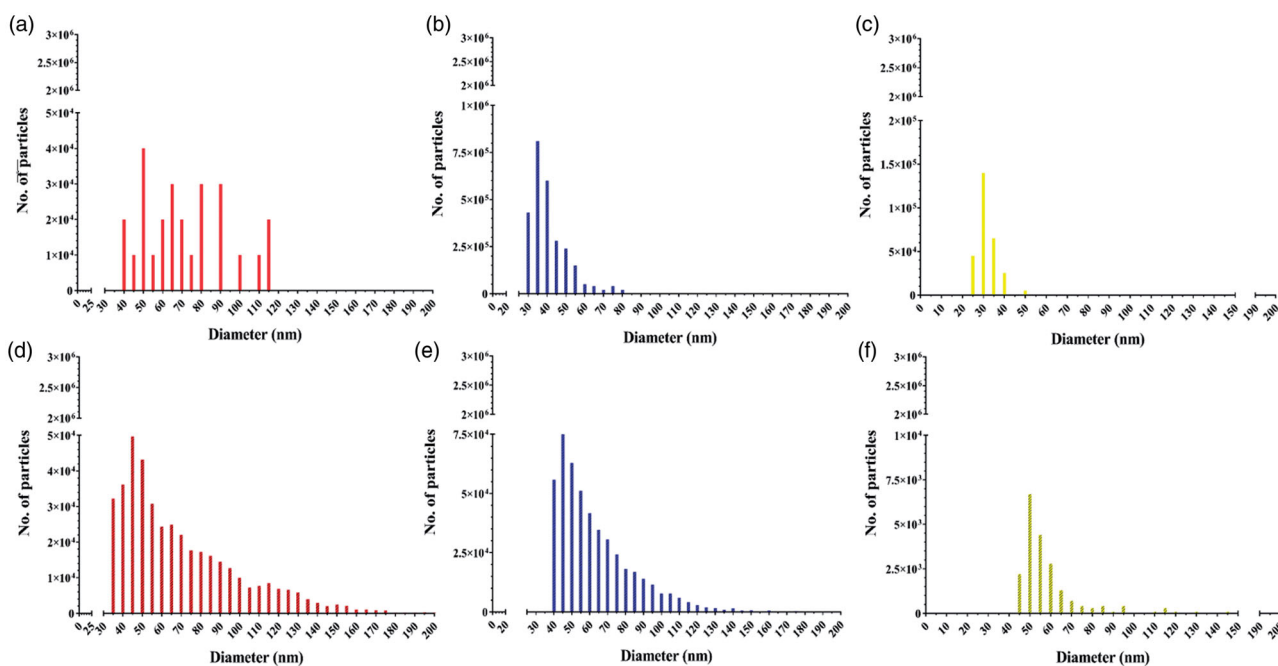


Figure 6. Number-weighted size distributions generated by spICP-MS measurement of Caco-2/HT29-MTX cellular silver content after 24 h exposure to (a) 500 $\mu\text{g/L}$ pristine (LA) AgNPs, (b) 500 $\mu\text{g/L}$ pristine 50 nm (Cit) AgNPs, (c) 250 $\mu\text{g/L}$ pristine AgNO_3 , (d) 500 $\mu\text{g/L}$ IVD (LA) AgNPs, (e) 500 $\mu\text{g/L}$ IVD (Cit) AgNPs, and (f) 250 $\mu\text{g/L}$ IVD AgNO_3 .

of 50 nm. Among IVD AgNPs, the number of NPs in the cell fraction exposed to (LA) AgNPs ($4.2 \times 10^5 \pm 3.6 \times 10^4$) was comparable to the number of particles detected in the cells exposed to (Cit) AgNPs ($4.4 \times 10^5 \pm 6 \times 10^4$).

The cellular fraction exposed to pristine AgNO₃ contained particulate Ag with a median size of 30 nm (Figure 6(c)), while the pristine AgNO₃ solution did not contain particles (Figure 5(c)). Upon exposure to IVD AgNO₃ solution, the cellular fraction contained silver particulates with a median size of 50 nm (Figures 5(f) and 6(F)). The number of particles measured in the cellular fraction upon exposure to AgNPs and AgNO₃ are presented in Supplementary Material, Table S1. All the size distributions of the three concentrations of AgNPs were following similar trend, accordingly all the size distributions reported in Figure 6 are only for of 500 µg/L of AgNPs and 250 µg/L AgNO₃ for simplicity and clarity purposes.

Discussion

This study aimed to investigate the impact of the different biochemical conditions within the human digestive tract – mimicked in *in vitro* incubations – on the intestinal fate and subsequent cellular uptake/association and passage across a monolayer of differentiated Caco-2/HT29-MTX intestinal cells. We observed that a significant fraction of the AgNPs dissolved after the *in vitro* digestion. Exposure of the monolayers of intestinal cells to increasing concentrations of pristine AgNPs resulted in a concentration dependent increase of total Ag and AgNPs contents in the cellular fractions. These concentrations were significantly lower following the exposure to the IVD AgNPs. Finally, passage of silver as total Ag or AgNPs was not detectable following the exposure to either pristine or IVD AgNPs.

The *in vitro* digestion model used here was adopted from the model described by Versantvoort et al. (Versantvoort et al. 2005; Walczak et al. 2012). The pH in the gastric digestion phase was set at 5 ± 0.5 to simulate the gastric environment upon ingestion of a meal (Gardner, Ciociola, and Robinson 2002; Minekus et al. 2014; Richardson and Feldman 1986). While this is the most realistic exposure scenario, it might underestimate the dissolution of AgNPs if consumed in fasted (empty

stomach) conditions, where the stomach pH is lower (pH 2) (Liu et al. 2012). Before *in vitro* digestion (i.e. the pristine suspensions), both AgNPs suspensions contained similar masses of total Ag and AgNPs, indicating that before *in vitro* digestion, the silver was present mainly in particulate form. In addition, the spICP-MS derived size distributions of both AgNPs suspensions were highly comparable.

Upon completion of all three digestion phases (oral, gastric and intestinal), the total Ag content in both of the IVD AgNPs suspensions and the AgNO₃ solution was similar to that of the corresponding pristine suspensions and solution, except for the highest concentration of both AgNPs, with the total Ag content being ~10% and ~40% lower for (LA) and (Cit) AgNPs, respectively. The reduction in total Ag content of samples taken from the highest concentrations could be due to a lower (analytical) recovery due to adsorption of AgNPs to the digestion matrix and tubing, and/or to the short centrifugation step applied to the AgNPs samples after digestion to spin down large protein precipitates before ICP-MS measurement (Versantvoort et al. 2005) to which the AgNPs could potentially adsorb (Noireaux et al. 2019). This centrifugation step is required to avoid the presence of large proteins that destabilize the plasma of the ICP-MS (Noireaux et al. 2019). On the other hand, a significant reduction in the mass- and number-based AgNPs content was observed for both AgNPs upon completion of all digestion phases, demonstrating that the *in vitro* digestion could induce dissolution, aggregation, or protein binding of the AgNPs (Böhmer et al. 2014). Significantly more of the (Cit) AgNPs endured the digestion conditions than the (LA) AgNPs, which is most likely due to the differences in surface chemistry of the AgNPs which is influencing the adsorption and agglomeration characteristics of the AgNPs. For example, the dissolution of (Cit) AgNPs in fresh river water was reported by Li and Lenhart to be much slower than that of tween coated AgNPs, where (Cit) AgNPs needed an incubation of 15 days to dissolve to the same extent as the tween coated AgNPs within 6 hours (Li and Lenhart 2012). Besides, in cell culture medium, (Cit) AgNPs have been shown to dissolve much slower compared to 5-kDa PEG-thiol-coated AgNPs (Zook et al. 2011). Dissolution of (LA)

coated AgNPs, reported in the present study, has not been studied before.

Interestingly, a significant number of silver particles was detected in the AgNO₃ solution after *in vitro* digestion, whereas in its pristine solution no particles were detected. The digestive juices have a high ionic strength including a high concentration of chloride, which is known to form particulate complexes with silver ions or the *de novo* formed AgNPs (Huynh and Chen 2011; Zook et al. 2011). This could explain the higher amount detected of cellular *de novo* formed AgNPs upon exposure to pristine AgNO₃ than exposure to IVD AgNO₃. Formation of *de novo* complexes of silver ions with chloride, sulfur or thiocyanate has been described before both *in vitro* (Kästner, Lampen, and Thünemann 2018; Walczak et al. 2012; Wildt et al. 2016) and *in vivo* (Levard et al. 2011; Loeschner et al. 2011).

In the present study, we used monolayers of differentiated Caco-2/HT29-MTX cells. The presence of mucus producing cells increases the physiological relevance of the model compared to using Caco-2 cells alone (Georgantzopoulou et al. 2015; Hilgendorf et al. 2000; Mahler, Shuler, and Glahn 2009; Yuan et al. 2013). Non-cytotoxic concentrations of AgNPs (and ionic controls) were used in our study. As chyme from the *in vitro* digestion model results in cytotoxic responses, the chyme was diluted in a 1:9 ratio with cell culture medium as described previously to avoid any cytotoxic effects (Böhmert et al. 2014; Lichtenstein et al. 2015; Walczak, Kramer, Hendriksen, Helsdingen, et al. 2015a).

After 24 hours of exposure to suspension of three concentrations of either pristine or IVD AgNPs, the total Ag and AgNPs contents of the cellular fraction increased in a concentration dependent manner. Both the total Ag and AgNPs contents in the cellular fractions were significantly lower following exposure to IVD AgNPs compared to the exposure to similar concentrations of pristine suspensions of AgNPs. Similar observations were reported for a differentiated Caco-2 cell model exposed to pristine and IVD AgNPs, although in that study only the total Ag content was measured (Lichtenstein et al. 2015). Furthermore, cellular uptake of total and particulate silver or titanium was also shown to be concentration dependent after 24 hours exposure in Neuro-2a cells (Hsiao et al. 2016).

The total Ag concentration found in the cellular fraction was in general higher than the AgNPs concentration, whereas upon digestion, the total Ag and AgNPs levels in the cellular fractions were highly comparable. As AgNPs tends to dissolve intracellularly (Singh and Ramarao 2012) and form protein corona upon IVD (Walczak, Kramer, Hendriksen, Helsdingen, et al. 2015a), it is likely that the *in vitro* digestion is protecting the AgNPs from dissolving inside the cells. In general, the AgNPs content in the cellular fraction appeared to be higher in the (LA) AgNPs samples than in the (Cit) AgNPs samples, following exposure to pristine AgNPs. The difference in the cellular total Ag content between (LA) and (Cit) AgNPs could be explained by possible formation of different types of protein coronas on the AgNPs due to their differences in surface chemistry, as previously described for AgNPs and other NPs (Abdelkhaliq et al. 2018; Lesniak et al. 2012; Monteiro-Riviere et al. 2013; Tenzer et al. 2013). Another factor influencing the interaction of AgNPs with cells could be the stability of the coating which might be affected by the ionic strength, protein content, or pH of the medium (Sharma et al. 2014).

Although spICP-MS is a very sensitive technique to quantify total Ag and AgNPs concentrations, it does not provide insights in the (sub)cellular localization of the Ag. Here, the confocal imaging showed that a fraction of the AgNPs was internalized in the cells.

Following exposure of the monolayers to AgNO₃ (pristine and IVD), AgNPs were detected in the cell fraction which suggests the *de novo* formation of AgNPs. However, the sizes of these AgNPs differed with a peak shift from 30 nm in the pristine samples to 50 nm in the digested samples. The *de novo* AgNPs are most likely to be firstly formed as silver salt complexes following the *in vitro* digestion and upon cellular exposure and internalization, these complexes may further interact with other cellular molecules rich in sulfur (*i.e.* cysteine and glutathione) and grow forming *de novo* nanoparticles *in situ* (Loeschner et al. 2011; Maurer et al. 2014; Wildt et al. 2016).

Lastly, we assessed the passage of total Ag and AgNPs across the monolayers of Caco-2/HT29-MTX cells. We performed all our experiments in transwells, and sampled the basolateral compartment following an exposure to both pristine and IVD AgNPs suspensions; the transport of silver as either

total Ag or AgNPs was < 0.1%. From an analytical perspective, the sensitivity and power of the methods used for detection and quantification of Ag and AgNPs (ICP-MS and spICP-MS respectively) were high compared to other methods that have been used before. That explains, why we could use low exposure concentrations (*i.e.* 250 µg/L), and still were able to detect total Ag and AgNPs in the cellular fractions. Other studies reported that the silver content in the cellular fractions after a higher exposure concentration (*i.e.* 1000 µg/L) of either pristine or IVD AgNO₃ solutions for the same exposure time was lower than the LOQ (20 µg/cm²) (Lichtenstein et al. 2015).

In addition, the basolateral samples were screened for AgNPs using TEM-EDS, but again no particles were detected. Previously, we have shown minimal passage (less than 1%) of smaller (20 nm) AgNPs across a monolayer of Caco-2/M-cells exposed for 4 h (Bouwmeester et al. 2011). For larger AgNPs it can be expected that the passage/transport is lower, in addition, we currently used membranes with a smaller pore size that might hinder the transport of the AgNPs (Cartwright et al. 2012). However, *in vivo* studies indicate that silver can reach the systemic circulation, as oral feeding studies with rodents have reported low oral bioavailability of silver after exposure to AgNPs of different sizes (Loeschner et al. 2011; van der Zande et al. 2012).

The Caco-2/HT29-MTX intestinal model shows potential for screening AgNPs. Addition of M-cells to the model is not of added value in the current case, as it was reported before to reduce the transport of NPs to a similar level of transport through Caco-2 monolayer where no mucus is present (Walczak, Kramer, Hendriksen, Tromp, et al. 2015b). In another study, AgNPs transport via a Caco-2/M-cell intestinal model could be detected (Bouwmeester et al. 2011) but the AgNPs used were of smaller size and in pristine status which might facilitate the possibility of detection. Applying longer exposure periods or higher non-toxic concentrations of AgNPs might increase the chance of detecting and quantifying transported AgNPs, owing to the limitation of the AgNPs stock concentration and the necessity to high dilution upon the digestion to avoid chyme toxicity. The broad spectrum of AgNPs with diverse physico-chemical characteristics might exhibit different

behaviors upon *in vitro* digestion and intestinal uptake and transport which highlight the importance of detailed characterization of AgNPs studied and the difficulty to group the AgNPs.

Conclusions

The surface chemistry of AgNPs had a significant influence on their dissolution and on their biological interactions with the Caco-2/HT29-MTX intestinal model. The (LA) AgNPs dissolved to a significantly higher extent during the digestion process compared to (Cit) AgNPs. Cellular uptake/association was in general higher for the (LA) AgNPs, although this difference disappeared after digestion. Upon *in vitro* digestion, the cellular uptake/association of both AgNPs decreased compared to the cellular uptake/association of pristine AgNPs. Transport of AgNPs across the monolayers of intestinal cells was < 0.1%. *De novo* formation of AgNPs was shown in the suspensions and in the cellular fractions upon digestion and cellular exposure of cells to AgNPs and AgNO₃.

The combination of *in vitro* digestion and intestinal barrier models used here confirms the interference and the influence of the digestion process on the biological interaction of the AgNPs upon oral ingestion. This highlights the need to take *in vitro* digestion into account when studying nanoparticle toxicokinetics and toxicodynamics in cellular *in vitro* model systems. Additionally, this combination is of added value to the safer-by-design NP development by identifying the physicochemical property (here the surface chemistry) that affects the uptake/association and cellular internalization.

Acknowledgments

The authors would like to thank Kerstin Jurkschat (Oxford University, UK) for TEM-EDS analysis.

Disclosure statement

The authors declare that they have no competing interests.

Funding

This work was supported by the NFP grant to AA and the EU H2020 project NanoFASE [grant no. 646002] to MZ, AU, and RP.

References

- Abdelkhalik, A., M. van der Zande, A. Punt, R. Helsdingen, S. Boeren, J. J. M. Vervoort, I. M. C. M. Rietjens, and H. Bouwmeester. 2018. "Impact of Nanoparticle Surface Functionalization on the Protein Corona and Cellular Adhesion, Uptake and Transport." *Journal of Nanobiotechnology* 16(1): 70. doi:10.1186/s12951-018-0394-6.
- Abdollahpur Monikh, F., L. Chupani, E. Zusková, R. Peters, M. Vancová, M. G. Vijver, P. Porcal, and W. J. G. M. Peijnenburg. 2019. "Method for Extraction and Quantification of Metal-Based Nanoparticles in Biological Media: Number-Based Biodistribution and Bioconcentration." *Environmental Science & Technology* 53: 946–953. doi:10.1021/acs.est.8b03715.
- Bailey, C. A., P. Bryla, and A. W. Malick. 1996. "The Use of the Intestinal Epithelial Cell Culture Model, Caco-2, in Pharmaceutical Development." *Advanced Drug Delivery Reviews* 22: 85–103. doi:10.1016/S0169-409X(96)00416-4.
- Böhmert, L., M. Girod, U. Hansen, R. Maul, P. Knappe, B. Niemann, S. M. Weidner, A. F. Thünemann, and A. Lampen. 2014. "Analytically Monitored Digestion of Silver Nanoparticles and Their Toxicity on Human Intestinal Cells." *Nanotoxicology* 8(6): 631–642. doi:10.3109/17435390.2013.815284.
- Bouwmeester, H., J. Poortman, R. J. Peters, E. Wijma, E. Kramer, S. Makama, K. Puspitaninganindita, H. J. P. Marvin, A. A. C. M. Peijnenburg, and P. J. M. Hendriksen. 2011. "Characterization of Translocation of Silver Nanoparticles and Effects on Whole-Genome Gene Expression Using an In Vitro Intestinal Epithelium Coculture Model." *ACS Nano* 5(5): 4091. doi:10.1021/nn2007145.
- Cartwright, L., M. S. Poulsen, H. M. Nielsen, G. Pojana, L. E. Knudsen, M. Saunders, and E. Rytting. 2012. "In Vitro Placental Model Optimization for Nanoparticle Transport studies." *International Journal of Nanomedicine* 7: 497–510. doi:10.2147/IJN.S26601.
- Chaudhry, Q., M. Scotter, J. Blackburn, B. Ross, A. Boxall, L. Castle, R. Aitken, and R. Watkins. 2008. "Applications and Implications of Nanotechnologies for the Food Sector." *Food Additives & Contaminants: Part A* 25: 241–258. doi:10.1080/02652030701744538.
- Choi, J. I., S. J. Chae, J. M. Kim, J. C. Choi, S. J. Park, H. J. Choi, H. Bae, and H. J. Park. 2018. "Potential Silver Nanoparticles Migration from Commercially Available Polymeric Baby Products into Food Simulants." *Food Additives & Contaminants: Part A* 35: 996–1005. doi:10.1080/19440049.2017.1411611.
- Ding, R., P. Yang, Y. Yang, Z. Yang, L. Luo, H. Li, and Q. Wang. 2018. "Characterisation of Silver Release from Nanoparticle-Treated Baby Products." *Food Additives & Contaminants: Part A* 35: 2052–2061. doi:10.1080/19440049.2018.1480064.
- Gardner, J. D., A. A. Ciociola, and M. Robinson. 2002. "Measurement of Meal-Stimulated Gastric Acid Secretion by In Vivo Gastric Autotitration." *Journal of Applied Physiology* 92(2): 427–434. doi:10.1152/jappphysiol.00956.2001.
- Georgantzopoulou, A., T. Serchi, S. Cambier, C. C. Leclercq, J. Renaut, J. Shao, M. Kruszewski, E. Lentzen, P. Grysan, S. Eswara, et al. 2015. "Effects of Silver Nanoparticles and Ions on a co-Culture Model for the Gastrointestinal Epithelium." *Particle and Fibre Toxicology* 13(1): 9. doi:10.1186/s12989-016-0117-9.
- Hilgendorf, C., H. Spahn-Langguth, C. G. Regårdh, E. Lipka, G. L. Amidon, and P. Langguth. 2000. "Caco-2 Versus Caco-2/HT29-MTX co-Cultured Cell Lines: Permeabilities via Diffusion, Inside- and Outside-Directed Carrier-Mediated Transport." *Journal of Pharmaceutical Sciences* 89(1): 63–75. doi:10.1002/(SICI)1520-6017(200001)89:1 <63::AID-JPS7 >3.0.CO;2-6.
- Hsiao, I. -L., F. S. Bierkandt, P. Reichardt, A. Luch, Y.-J. Huang, N. Jakubowski, J. Tentschert, and A. Haase. 2016. "Quantification and Visualization of Cellular Uptake of TiO₂ and Ag Nanoparticles: Comparison of Different ICP-MS Techniques." *Journal of Nanobiotechnology* 14(1): 50. doi:10.1186/s12951-016-0203-z.
- Huynh, K. A., and K. L. Chen. 2011. "Aggregation Kinetics of Citrate and Polyvinylpyrrolidone Coated Silver Nanoparticles in Monovalent and Divalent Electrolyte Solutions." *Environmental Science & Technology* 45: 5564–5571. doi:10.1021/es200157h.
- Imai, S., Y. Morishita, T. Hata, M. Kondoh, K. Yagi, J. -Q. Gao, K. Nagano, K. Higashisaka, Y. Yoshioka, and Y. Tsutsumi. 2017. "Cellular Internalization, Transcellular Transport, and Cellular Effects of Silver Nanoparticles in Polarized Caco-2 Cells Following Apical or Basolateral Exposure." *Biochemical and Biophysical Research Communications* 484(3): 543–549. doi:10.1016/j.bbrc.2017.01.114.
- Kästner, C., A. Lampen, and A. F. Thünemann. 2018. "What Happens to the Silver Ions? – Silver Thiocyanate Nanoparticle Formation in an Artificial Digestion." *Nanoscale* 10(8): 3650–3653. doi:10.1039/C7NR08851E.
- Kittler, S., C. Greulich, J. Diendorf, M. Köller, and M. Epple. 2010. "Toxicity of Silver Nanoparticles Increases During Storage Because of Slow Dissolution under Release of Silver Ions." *Chemistry of Materials* 22(16): 4548–4554. doi:10.1021/cm100023p.
- Kleiveland, C. R. 2015. "Co-Cultivation of Caco-2 and HT-29MTX." In *The Impact of Food Bioactives on Health: In Vitro and Ex Vivo Models*, edited by K Verhoeckx, P Cotter, I López-Expósito, C Kleiveland, T Lea, A Mackie, T Requena, D Swiatecka, H Wichers, 135–140. Cham: Springer International Publishing.
- Laborda, F., J. Jimenez-Lamana, E. Bolea, and J. R. Castillo. 2011. "Selective Identification, Characterization and Determination of Dissolved Silver(i) and Silver Nanoparticles Based on Single Particle Detection by Inductively Coupled Plasma Mass Spectrometry." *Journal of Analytical Atomic Spectrometry* 26(7): 1362–1371. doi:10.1039/c0ja00098a.
- Lefebvre, D. E., K. Venema, L. Gombau, L. G. Valerio, J. Raju, G. S. Bondy, H. Bouwmeester, R. P. Singh, A. J. Clippinger,

- E-M. Collnot, et al. 2015. "Utility of Models of the Gastrointestinal Tract for Assessment of the Digestion and Absorption of Engineered Nanomaterials Released from Food Matrices." *Nanotoxicology* 9(4): 523–542. doi:10.3109/17435390.2014.948091.
- Lesniak, A., F. Fenaroli, M. P. Monopoli, C. Åberg, K. A. Dawson, and A. Salvati. 2012. "Effects of the Presence or Absence of a Protein Corona on Silica Nanoparticle Uptake and Impact on Cells." *ACS Nano* 6(7): 5845–5857. doi:10.1021/nn300223w.
- Levard, C., B. C. Reinsch, F. M. Michel, C. Oumahi, G. V. Lowry, and G. E. Brown. 2011. "Sulfidation Processes of PVP-Coated Silver Nanoparticles in Aqueous Solution: Impact on Dissolution Rate." *Environmental Science & Technology* 45: 5260–5266. doi:10.1021/es2007758.
- Li, X., and J. J. Lenhart. 2012. "Aggregation and Dissolution of Silver Nanoparticles in Natural Surface Water." *Environmental Science & Technology* 46: 5378–5386. doi:10.1021/es204531y.
- Lichtenstein, D., J. Ebmeyer, P. Knappe, S. Juling, L. Böhmert, S. Selve, B. Niemann, A. Braeuning, A. F. Thünemann, and A. Lampen. 2015. "Impact of Food Components During In Vitro Digestion of Silver Nanoparticles on Cellular Uptake and Cytotoxicity in Intestinal Cells." *Biological Chemistry* 396(11): 1255. doi:10.1515/hsz-2015-0145.
- Lichtenstein, D., J. Ebmeyer, T. Meyer, A. -C. Behr, C. Kästner, L. Böhmert, S. Juling, B. Niemann, C. Fahrenson, S. Selve, et al. 2017. "It Takes More than a Coating to Get Nanoparticles Through the Intestinal Barrier In Vitro." *European Journal of Pharmaceutics and Biopharmaceutics* 118: 21–29. doi:10.1016/j.ejpb.2016.12.004.
- Liu, J., Z. Wang, F. D. Liu, A. B. Kane, and R. H. Hurt. 2012. "Chemical Transformations of Nanosilver in Biological Environments." *ACS Nano* 6(11): 9887–9899. doi:10.1021/nn303449n.
- Loeschner, K., N. Hadrup, K. Qvortrup, A. Larsen, X. Gao, U. Vogel, A. Mortensen, H. R. Lam, and E. H. Larsen. 2011. "Distribution of Silver in Rats following 28 Days of Repeated Oral Exposure to Silver Nanoparticles or Silver Acetate." *Particle and Fibre Toxicology* 8(1): 18. doi:10.1186/1743-8977-8-18.
- López-Serrano, A., R. M. Olivas, J. S. Landaluze, and C. Cámara. 2014. "Nanoparticles: A Global Vision. Characterization, Separation, and Quantification Methods. Potential Environmental and Health Impact." *Analytical Methods* 6(1): 38–56. doi:10.1039/C3AY40517F.
- Mahler, G. J., M. L. Shuler, and R. P. Glahn. 2009. "Characterization of Caco-2 and HT29-MTX Cocultures in an In Vitro Digestion/Cell Culture Model Used to Predict Iron Bioavailability." *Journal of Nutritional Biochemistry* 20(7): 494–502. doi:10.1016/j.jnutbio.2008.05.006.
- Maurer, E. I., M. Sharma, J. J. Schlager, and S. M. Hussain. 2014. "Systematic Analysis of Silver Nanoparticle Ionic Dissolution by Tangential Flow Filtration: Toxicological Implications." *Nanotoxicology* 8: 718–727. doi:10.3109/17435390.2013.824127.
- McCracken, C., A. Zane, D. A. Knight, E. Hommel, P. K. Dutta, and W. J. Waldman. 2015. "Oxidative Stress-Mediated Inhibition of Intestinal Epithelial Cell Proliferation by Silver Nanoparticles." *Toxicology In Vitro* 29(7): 1793–1808. doi:10.1016/j.tiv.2015.07.017.
- Minekus, M., M. Alminger, P. Alvito, S. Ballance, T. Bohn, C. Bourlieu, F. Carrière, R. Boutrou, M. Corredig, D. Dupont, et al. 2014. "A Standardised Static In Vitro Digestion Method Suitable for Food – An International Consensus." *Food & Function* 5: 1113–1124. doi:10.1039/C3FO60702J.
- Monteiro-Riviere, N. A., M. E. Samberg, S. J. Oldenburg, and J. E. Riviere. 2013. "Protein Binding Modulates the Cellular Uptake of Silver Nanoparticles into Human Cells: Implications for In Vitro to In Vivo Extrapolations?" *Toxicology Letters* 220(3): 286–293. doi:10.1016/j.toxlet.2013.04.022.
- Murdock, R. C., L. Braydich-Stolle, A. M. Schrand, J. J. Schlager, and S. M. Hussain. 2008. "Characterization of Nanomaterial Dispersion in Solution Prior to In Vitro Exposure Using Dynamic Light Scattering Technique." *Toxicological Sciences* 101(2): 239–253. doi:10.1093/toxsci/kfm240.
- Mwilu, S. K., A. M. El Badawy, K. Bradham, C. Nelson, D. Thomas, K. G. Scheckel, T. Tolaymat, L. Ma, and K. R. Rogers. 2013. "Changes in Silver Nanoparticles Exposed to Human Synthetic Stomach Fluid: Effects of Particle Size and Surface Chemistry." *Science of the Total Environment* 447: 90–98. doi:10.1016/j.scitotenv.2012.12.036.
- Nel, A., T. Xia, L. Mädler, and N. Li. 2006. "Toxic Potential of Materials at the Nanolevel." *Science* 311(5761): 622–627. doi:10.1126/science.1114397.
- Noireaux, J., R. Grall, M. Hullo, S. Chevillard, C. Oster, E. Brun, C. Sicard-Roselli, K. Loeschner, and P. Fiscaro. 2019. "Gold Nanoparticle Uptake in Tumor Cells: Quantification and Size Distribution by sp-ICPMS." *Separations* 6(1): 3. doi:10.3390/separations6010003.
- Peters, R., Z. Herrera-Rivera, A. Undas, M. van der Lee, H. Marvin, H. Bouwmeester, and S. Weigel. 2015. "Single Particle ICP-MS Combined with a Data Evaluation Tool as a Routine Technique for the Analysis of Nanoparticles in Complex Matrices." *Journal of Analytical Atomic Spectrometry* 30(6): 1274–1285. doi:10.1039/C4JA00357H.
- Richardson, C. T., and M. Feldman. 1986. "Salivary Response to Food in Humans and Its Effect on Gastric Acid Secretion." *American Journal of Physiology-Gastrointestinal and Liver Physiology* 250(1): G85–G91. doi:10.1152/ajpgi.1986.250.1.G85.
- Sharma, V. K., K. M. Siskova, R. Zboril, and J. L. Gardea-Torresdey. 2014. "Organic-Coated Silver Nanoparticles in Biological and Environmental Conditions: Fate, Stability and Toxicity." *Advances in Colloid and Interface Science* 204: 15–34. doi:10.1016/j.cis.2013.12.002.
- Sieg, H., C. Kästner, B. Krause, T. Meyer, A. Burel, L. Böhmert, D. Lichtenstein, H. Jungnickel, J. Tentschert, P. Laux, et al. 2017. "Impact of an Artificial Digestion Procedure on Aluminum-Containing Nanomaterials." *Langmuir* 33(40): 10726–10735. doi:10.1021/acs.langmuir.7b02729.

- Singh, R. P., and P. Ramarao. 2012. "Cellular Uptake, Intracellular Trafficking and Cytotoxicity of Silver Nanoparticles." *Toxicology Letters* 213(2): 249–259. doi:10.1016/j.toxlet.2012.07.009.
- Stone, V., H. Johnston, and R. P. F. Schins. 2009. "Development of In Vitro Systems for Nanotoxicology: Methodological Considerations." *Critical Reviews in Toxicology* 39(7): 613–626. doi:10.1080/10408440903120975.
- Tenzer, S., D. Docter, J. Kuharev, A. Musyanovych, V. Fetz, R. Hecht, F. Schlenk, D. Fischer, K. Kiouptsi, C. Reinhardt, et al. 2013. "Rapid Formation of Plasma Protein Corona Critically Affects Nanoparticle Pathophysiology." *Nature Nanotechnology* 8(10): 772–781.
- van der Zande, M., A. K. Undas, E. Kramer, M. P. Monopoli, R. J. Peters, D. Garry, E. C. Antunes Fernandes, P. J. Hendriksen, H. J. P. Marvin, A. A. Peijnenburg, et al. 2016. "Different Responses of Caco-2 and MCF-7 Cells to Silver Nanoparticles Are Based on Highly Similar Mechanisms of Action." *Nanotoxicology* 10(10): 1431–1441. doi:10.1080/17435390.2016.1225132.
- van der Zande, M., R. J. Vandebriel, E. Van Doren, E. Kramer, Z. Herrera Rivera, C. S. Serrano-Rojero, E. R. Gremmer, J. Mast, R. J. B. Peters, P. C. H. Hollman., et al. 2012. "Distribution, Elimination, and Toxicity of Silver Nanoparticles and Silver Ions in Rats after 28-Day Oral Exposure." *ACS Nano* 6(8): 7427–7442. doi:10.1021/nn302649p.
- Versantvoort, C. H. M., A. G. Oomen, E. Van de Kamp, C. J. M. Rempelberg, and A. J. A. M. Sips. 2005. "Applicability of an In Vitro Digestion Model in Assessing the Bioaccessibility of Mycotoxins from Food." *Food and Chemical Toxicology* 43(1): 31–40. doi:10.1016/j.fct.2004.08.007.
- Walczak, A. P., R. Fokink, R. Peters, P. Tromp, Z. E. Herrera Rivera, I. M.C.M. Rietjens, P. J.M. Hendriksen, and H. Bouwmeester. 2012. "Behaviour of Silver Nanoparticles and Silver Ions in an In Vitro Human Gastrointestinal Digestion Model." *Nanotoxicology* 7(7): 1198–1210. doi:10.3109/17435390.2012.726382.
- Walczak, A. P., E. Kramer, P. J. M. Hendriksen, R. Helsdingen, M. van der Zande, I. M. C. M. Rietjens, and H. Bouwmeester. 2015. "In Vitro Gastrointestinal Digestion Increases the Translocation of Polystyrene Nanoparticles in an In Vitro Intestinal Co-Culture Model." *Nanotoxicology* 9(7): 886–894. doi:10.3109/17435390.2014.988664.
- Walczak, A. P., E. Kramer, P. J. M. Hendriksen, P. Tromp, J. P. F. G. Helsper, M. van der Zande, I. M. C. M. Rietjens, and H. Bouwmeester. 2015. "Translocation of Differently Sized and Charged Polystyrene Nanoparticles in In Vitro Intestinal Cell Models of Increasing Complexity." *Nanotoxicology* 9(4): 453–461. doi:10.3109/17435390.2014.944599.
- Weigel, S., R. Peters, K. Loeschner, R. Grombe, and T. P. J. Linsinger. 2017. "Results of an Interlaboratory Method Performance Study for the Size Determination and Quantification of Silver Nanoparticles in Chicken Meat by Single-Particle Inductively Coupled Plasma Mass Spectrometry (sp-ICP-MS)." *Analytical and Bioanalytical Chemistry* 409(20): 4839–4848. doi:10.1007/s00216-017-0427-2.
- Wildt, B. E., A. Celedon, E. I. Maurer, B. J. Casey, A. M. Nagy, S. M. Hussain, and P. L. Goering. 2016. "Intracellular Accumulation and Dissolution of Silver Nanoparticles in L-929 Fibroblast Cells Using Live Cell Time-Lapse Microscopy." *Nanotoxicology* 10(6): 710–719. doi:10.3109/17435390.2015.1113321.
- Yuan, H., C. Chen, G. Chai, Y. Du, and F. Hu. 2013. "Improved Transport and Absorption through Gastrointestinal Tract by PEGylated Solid Lipid Nanoparticles." *Molecular Pharmaceutics* 10(5): 1865–1873.
- Zook, J. M., S. E. Long, D. Cleveland, C. L. A. Geronimo, and R. I. MacCuspie. 2011. "Measuring Silver Nanoparticle Dissolution in Complex Biological and Environmental Matrices Using UV-Visible Absorbance." *Analytical and Bioanalytical Chemistry* 401(6): 1993. doi:10.1007/s00216-011-5266-y.